A Model of Movement Coordinates in the Motor Cortex: Posture-dependent Changes in the Gain and Direction of Single Cell Tuning Curves

Robert Ajemian, Daniel Bullock and Stephen Grossberg

Department of Cognitive and Neural Systems, and Center for Adaptive Systems, Boston University, 677 Beacon Street, Boston, MA 02215, USA

This article outlines a methodology for investigating the coordinate systems by which movement variables are encoded in the firing rates of individual motor cortical neurons. Recent neurophysiological experiments have probed the issue of underlying coordinates by examining how cellular preferred directions (as determined by the center-out task) change with posture. Several key experimental findings have resulted that constrain hypotheses about how motor cortical cells encode movement information. But while the significance of shifts in preferred direction is well known and widely accepted, posture-dependent changes in the depth of modulation of a cell's tuning curve — that is, gain changes — have not been similarly identified as a means of coordinate inference. This article develops a vector field framework in which the preferred direction and the gain of a cell's tuning curve are viewed as dual components of a unitary response vector. The formalism can be used to compute how each aspect of cell response covaries with posture as a function of the coordinate system in which a given cell is hypothesized to encode its movement information. Such an integrated approach leads to a model of motor cortical cell activity that codifies the following four observations: (i) cell activity correlates with hand movement direction; (ii) cell activity correlates with hand movement speed; (iii) preferred directions vary with posture; and (iv) the modulation depth of tuning curves varies with posture. Finally, the model suggests general methods for testing coordinate hypotheses at the single-cell level and simulates an example protocol for three possible coordinate systems: Cartesian spatial, shoulder-centered, and joint angle.

Introduction

The activity of neurons in the primary motor cortex (M1) of primates has been shown to correlate with multiple kinematic and kinetic parameters of multi-joint movement: direction (Georgopoulos *et al.*, 1982; Schwartz *et al.*, 1988; Ashe and Georgopoulos, 1994), movement speed (Schwartz, 1992; Ashe and Georgopoulos, 1994; Moran and Schwartz, 1999a), hand position (Georgopoulos *et al.*, 1984; Kettner *et al.*, 1988; Ashe and Georgopoulos, 1994), movement amplitude (Fu *et al.*, 1993, 1995), arm posture (Scott and Kalaska, 1997), force (Kalaska and Hyde, 1985; Kalaska *et al.*, 1989; Georgopoulos *et al.*, 1992; Taira *et al.*, 1996; Sergio and Kalaska, 1997, 1998) and target direction (Alexander and Crutcher, 1990b; Shen and Alexander, 1997), among others. Further complicating the role of M1 in motor behavior are established correlations with aspects of movement planning such as movement preparation (Alexander and Crutcher, 1990a; Kettner and Marcario, 1996), target sequence information (Carpenter *et al.*, 1999), and rapid motor adaptation (Wise *et al.*, 1998). Cell activity in M1, therefore, shows relations to a multitude of movement variables that span the sensorimotor spectrum.

Given that cells exhibit differing response sensitivities to these variables, it makes sense to delineate, as much as possible, distinct components of cell response for the purpose of identifying which variables are prominently represented by which cells. With this information, one can begin to understand how movement commands are assembled in the cortex. However, the knowledge that a specific movement variable is encoded in a given cell's response does not fully specify the nature of the underlying representation, because a movement variable can be encoded in any of several possible coordinate systems. For example, movement direction can be represented as a spatial direction (Cartesian spatial coordinates), a combination of joint angle rotations (joint angle coordinates), or a collection of muscle length changes (muscle-space coordinates). The encoding of force using these same three coordinate systems results in the alternative descriptions of Cartesian end-point forces, joint torques, and muscle forces. Static variables, too, such as hand position in space, can be encoded in different coordinate systems (Lacquaniti *et al.*, 1995). Against this backdrop of manifold coordinate possibilities, it is critical to disambiguate between alternative coordinate representations of the same movement variable, because such distinctions constrain hypotheses about a cell's role in the overall motor circuit.

The problem of determining an underlying coordinate system for the encoding of specific movement information can be referred to as the *coordinate inference problem*. This paper develops a combination of analytic techniques and experimental strategies for solving this problem on the basis of cell response properties as observed across different motor contexts. The analysis is conducted at the single-cell level, since brain regions do not appear to be homogeneous with respect to coordinate representation (Crutcher and Alexander, 1990). The methods in this paper, though more generally applicable, focus on the encoding of two movement variables, *movement direction* and *movement speed*, which together constitute a unitary physical entity: the velocity vector. These two variables of motion are robustly represented in the activity of individual M1 cells (Georgopoulos *et al.*, 1982; Schwartz *et al.*, 1988; Schwartz, 1992; Ashe and Georgopoulos, 1994; Moran and Schwartz, 1999a).

With regard to the encoding of movement direction, a single instance of a cell's preferred direction, determined within a small region of space, cannot support a coordinate inference since all coordinate descriptions are equally valid locally (Mussa-Ivaldi, 1988). Therefore, multiple preferred directions, drawn from distinct workspace positions and/or arm postures, have been utilized in attempts to distinguish between coordinate systems (Caminiti *et al.*, 1990; Scott and Kalaska, 1997; Kakei *et al.*, 1999). But while a cell's preferred direction has been identified as a context-dependent response feature important for adducing coordinates, the depth of modulation of a cell's tuning curve — that is, a cell's *gain* — has gone essentially unrecognized as bearing on the coordinate inference problem. Few interpretations have been offered as to what a motor cortical cell's gain

Cerebral Cortex Dec 2001;11:1124–1135; 1047–3211/01/$4.00

represents or why cellular gains are observed to change with posture (Caminiti *et al.*, 1990; Scott and Kalaska, 1997; Kakei *et al.*, 1999). Our vector field framework, in which a cell's gain is interpreted as a response property coupled to the cell's preferred direction, suggests how gain changes signify underlying coordinate representations and thus can play a critical role in solving the coordinate inference problem. This interpretation of cellular gain leads to a model of motor cortical activity that offers a parsimonious explanation of the dependency of cell firing rates on both movement direction and movement speed.

Methods

Model and Approach

An M1 cell's directional tuning curve, as derived from the standard center-out task (Georgopoulos *et al.*, 1982), relates the average movement-related cell activity to the hand movement direction:

$$\upsilon(\omega) = b_0 + b_1 \cos(\omega - \omega_{pd}) \quad (1)$$

where υ is the cell's firing rate, ω is the hand movement direction, b_0 is the average movement-related response, b_1 is the amplitude or depth of modulation of the tuning curve, and ω_{pd} is the preferred direction (pd), that is, the movement direction in space that elicits the maximal cellular response. Georgopoulos *et al.* (1982) showed that the cosine tuning model resulted in a good fit for the activity modulation of many M1 neurons. The distribution of preferred directions (pds) across a population of cells has been found to span the continuum of possible movement directions (Georgopoulos *et al.*, 1982; Schwartz *et al.*, 1988). These two results could be considered to suggest that movement direction is encoded in a Cartesian spatial coordinate system. However, Mussa-Ivaldi (1988) showed that cosine tuning would arise even if motor cortical cell activity is linearly related to the time rate of change of multiple muscle lengths. Thus, spatial tuning does not necessarily imply a spatial coordinate representation. Findings that pds vary with position (Caminiti *et al.*, 1990) and posture (Caminiti *et al.*, 1990; Scott and Kalaska, 1997) further complicate the notion of a spatial representation. So far, no consensus has emerged on the issue of coordinates, and a variety of reference frames covering the sensorimotor spectrum have been proposed to interpret M1 cell activity (Bullock and Grossberg, 1988; Mussa-Ivaldi, 1988; Caminiti *et al.*, 1990; Schwartz, 1992; Sanger, 1994; Tanaka, 1994; Scott and Kalaska, 1997; Kakei *et al.*, 1999; Zhang and Sejnowski, 1999; Ajemian *et al.*, 2000; Todorov, 2000).

Analysis of the coordinate inference problem motivates an explicit distinction between a representation of preferred direction as it is measured in the coordinate system utilized by the experimentalist, the *spatial pd*, and direction as it exists in the coordinate system in which a cell operates by virtue of its placement in the nervous system, the *internal pd*. Whereas a spatial pd determination arises naturally from the fact that experiments are performed and calibrated in extrapersonal space, determining a corresponding internal pd requires additional steps. These steps involve the transformations that convert back and forth between alternative coordinate descriptions of the same underlying directional entity. Using these transformations as well as the distinction between an internal pd and a spatial pd, Ajemian *et al.* (Ajemian *et al.*, 2000) developed a vector field framework for investigating the issue of coordinate systems. The original formulation addressed posture-dependent shifts in a cell's spatial pd. We will briefly summarize those results in the next section before extending the method to address posture-dependent changes in the depth of modulation of a cell's tuning curve and the dependence of cell firing rates on hand speed.

The Model Arm

Analyses in this paper assume a standard two-joint or two-degree-of-freedom (2-DOF) arm moving on a planar workspace situated within the horizontal plane passing through the shoulder (Fig. 1*A*) – see the Appendix for a mathematical description of the arm. A critical feature of the 2-DOF planar arm that simplifies our analysis is that hand positions map one-to-one to arm postures. Thus, the terms 'hand position' and 'arm

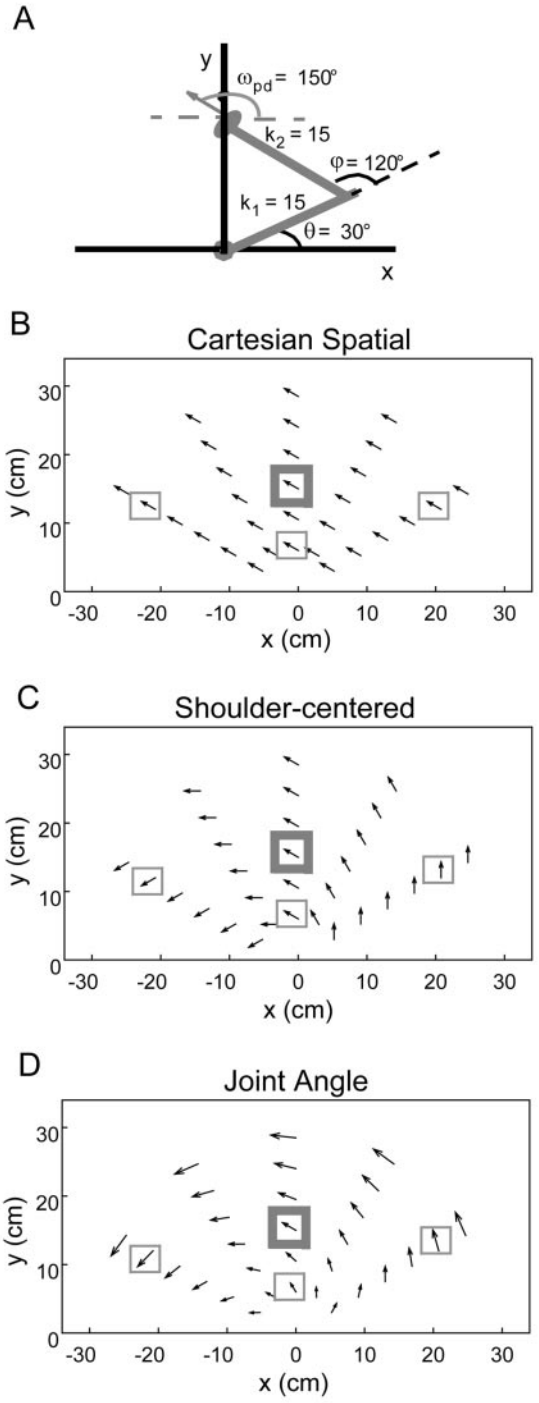

Figure 1. Generating vector fields of spatial pds. (*A*) The 2-DOF planar arm at the reference posture of $(\theta, \varphi) = (30°, 120°)$ corresponding to an end-effector location of $(x, y) = (0, 15)$. The upper and lower arm lengths are taken to be 15 cm. The spatial pd for the sample cell at the reference posture is 150°. (*B*) Vector field of spatial pds for the sample cell under the assumption of Cartesian spatial coordinates. The spatial pd at the reference posture is contained in the thick gray box for this and the remaining vector field plots. All the other arrows are predictions of the spatial pds at other locations based on the coordinate hypothesis. The arrows surrounded by the thin boxes are sample spatial pd vector predictions that could be highlighted by the direct sampling method (see Results). For this coordinate system, spatial pds remain constant across the workspace. (*C*) Vector field of spatial pds under the assumption of shoulder-centered coordinates. Spatial pds change across the workspace in accord with the shoulder rotation. (*D*) Vector field of spatial pds under the assumption of joint angle coordinates. Spatial pds change across the workspace in a pattern that distinctly differs from either of the other two coordinate systems. Only here do the magnitudes of the vectors change as well as the direction.

posture' can be freely interchanged since the former uniquely defines the latter, a situation that does not hold for motor redundant arms.

Vector Fields of Spatial pds

Given a spatial pd at only one posture, all coordinate descriptions are equally valid and the coordinate inference problem is ill-posed. For example, suppose at some reference posture that a cell's spatial pd is measured as 30°. That movement direction in space can, through an appropriate transformation, be converted into a movement direction in any well-defined internal space: for joint angle coordinates, the 30° in space can be converted into a ratio of joint angle rotations; for muscle-length coordinates, the 30° in space can be converted into a ratio of muscle-length changes; and so on for any explicitly defined coordinate system.

However, because the transformation between movement directions in the internal space and movement directions in external space is in general *posture dependent*, additional constraints can be imposed by spatial pd estimates obtained at multiple postures. Provided that a cell's internal pd is fixed (if, for example, a cell encodes a fixed ratio of joint angle velocities), then knowing its spatial pd at one posture allows unique predictions of the cell's corresponding spatial pd at all other postures in the workspace. This strategy is outlined in a four-step vector field method for distinguishing between coordinate systems:

1. Measure a cell's spatial pd at a reference posture.
2. Choose an internal coordinate system and map the cell's spatial pd from step 1 to an internal pd using the transformation appropriate for the chosen coordinate system.
3. Select a new posture and convert the internal pd from step 2 into a corresponding spatial pd using the reverse transformation between directions in the two spaces. Because of its posture dependence, this transformation will, in general, no longer be simply the inverse of the transformation in step 2. Therefore, the new spatial pd will, in general, differ from the spatial pd at the reference posture, even though the internal pd is constant.
4. Using the internal pd from step 2, repeat step 3 for postures that sample the entire workspace of the 2-DOF planar arm. Determining a direction and a magnitude over a field of points yields a *vector field* of spatial pds. For a given cell, each coordinate-dependent vector field constitutes a set of predictions that can be compared to actual measurements to choose a coordinate system of best fit.

The type of coordinate analysis contained in the steps above belongs to the branch of mathematics known as differential geometry.

Results

In Figure 1*B–D*, we plot vector fields of spatial pds for three internal coordinate systems: Cartesian spatial, shoulder-centered, and joint angle. In each case, a cell's preferred direction at a single reference posture has been extrapolated into distinct vector fields of spatial pds as a function of coordinate hypothesis. The plots shown are based on a simulated sample cell that has a spatial pd of 150° at the reference posture (see Fig. 1*A*). For a mathematical description of these coordinate systems in the context of the 2-DOF arm as well as empirical motivations for their usage, see the Appendix or Ajemian *et al*. (Ajemian *et al*., 2000).

Gain Changes

Vectors possess a magnitude in addition to a direction. Since coordinate transformations in general show posture-dependent *scaling* effects as well as directional effects, the length of spatial pd vectors, as computed in the four-step procedure above, may vary across the workspace (see Fig. 1*D*). What, then, is the physiological interpretation of spatial pd vector magnitude? Apart from a cell's preferred direction, the depth of modulation of a cell's tuning curve, denoted by b_1 in equation (1), is another important response feature. Hereafter, this b_1 term will be referred to as the cellular *gain* because it scales the directional component of cell activity. Just as the direction of a spatial pd vector represents the direction to which a cell is tuned, the magnitude of a spatial pd vector represents the degree to which the cell is tuned, that is, the gain of the response. Specifically, a cell's gain at any given posture is directly proportional to the magnitude of the spatial pd vector at that posture. With this gain interpretation incorporated into our vector field formalism, a spatial pd vector embodies two aspects of cell response: the vector direction corresponds to the spatial pd and the vector magnitude corresponds to the gain. The mathematical model thus allows a cell's spatial pd and gain measured at a reference posture to be converted into coordinate-dependent predictions of the spatial pd and gain at all postures.

Intuitively, the link between spatial pd vector magnitude and cellular gains can be explained as follows. Suppose that a cell is tuned to a joint synergy in its internal space. At some postures, a fixed joint displacement in the direction of that synergy will transform into a relatively large spatial displacement of the hand; at other postures, the same joint displacement will lead to a relatively small hand displacement. In those postures where the cell's preferred joint synergy is particularly effective at inducing hand motion, the cell will be prominently recruited as a significant contributor to movement and the cell's directional activity will be heavily modulated. Conversely, a cell will exhibit little directional modulation in postures where its preferred joint synergy is ineffectual at generating hand motion. Thus, according to our hypothesis, variable gains reflect the fact that cell modulation *scales* with the biomechanical advantage of the 'action' controlled by the cell. This idea is compatible with findings that the pattern of EMG activity in many muscles, including the depth of EMG modulation across movement directions, changes when the center-out task is performed at different positions/postures in the workspace (Caminiti *et al*., 1990; Scott and Kalaska, 1997; Kakei *et al*., 1999). Presumably, the differentiated pattern of muscle recruitment stems, at least in part, from posture-dependent alterations in a muscle's biomechanical advantage. If M1 cells are viewed as controlling relatively fixed motor synergies, then their activity should be modulated by posture according to the same principle.

In Scott and Kalaska (Scott and Kalaska 1997), where the center-out task was performed in a natural and an abducted posture, a majority (53%) of cells showed statistically significant gain changes between postures. Kakei *et al*. looked at the preferred directions of wrist-related M1 cells in three postures and found that a majority (63.3%) of cells demonstrated gain changes of greater than 30% across postures (Kakei *et al*., 1999). Vector field analysis suggests that the observed widespread variability in cellular gain may result from encoding in a coordinate system, such that the transformation into spatial coordinates exhibits similarly pronounced posture-dependent scaling effects. This hypothesis can be tested by modeling pertinent joint-based or muscle-based coordinate systems.

The data also show that directional tuning itself occurs in a posture-dependent fashion: Caminiti *et al*. and Scott and Kalaska reported cells that were tuned in one posture/position but not in another (Caminiti *et al*., 1990; Scott and Kalaska, 1997). In Caminiti *et al*., where the center-out task was performed from three different workspace locations, 25% of the cells were tuned in either one or two locations but not all three (Caminiti *et al*., 1990). This loss of discernible directional tuning need not result from an unspecified switching process in which cells are actively tuned only in a certain postural region; instead, the phenomenon of posture-dependent tuning may be accounted for

more naturally as posture-dependent gain attenuation below the threshold required to make a determination of statistically significant directional modulation. Therefore, we suggest that those cells that lose their directional modulation in one or more postures are displaying gain changes of an extreme type.

For the three internal coordinate systems used in this study, investigation of posture-dependent gain changes yields several contrasting conclusions. Neither Cartesian spatial cells nor shoulder-centered cells will exhibit gain changes since neither the identity transformation (associated with Cartesian spatial coordinates) nor the rotational transformation (associated with shoulder-centered coordinates) engenders posture-dependent scaling effects. However, cells coding joint angle coordinates will exhibit significant gain changes across the workspace, because the Jacobian transformation introduces significant posture-dependent scaling effects, which can be observed for our sample cell as vector length variations in Figure 1*D*. The Appendix mathematically analyzes the scaling effects of the Jacobian to derive an explicit expression for a cell's gain at an arbitrary point in the workspace as a function of that cell's gain at a reference posture. This analysis leads to four experimental predictions.

1. For all cells, the gain is a monotonically varying function of the shoulder-to-hand distance, *r*, either increasing or decreasing, with no additional dependence on the Cartesian position coordinates *x* or *y* considered separately.
2. The variation in gain systematically depends upon the joint synergy to which the cell is tuned. For example, when the shoulder component of a cell's joint synergy is large relative to the elbow component, the gain changes will be large; conversely, when the elbow component is large relative to the shoulder component, the gain changes will be small. Table 1 shows the link between a cell's joint synergy and predicted gain changes for a few sample cells.
3. Since a cell's spatial pd at a reference posture maps to a joint synergy and since a joint synergy maps to specific gain changes, a cell's spatial pd at a reference posture can be mapped to the gain changes that cell is predicted to undergo. Such a mapping, depicted in Figure 2, constitutes a novel experimental prediction of the coupling between spatial pd values and gain changes.
4. The population statistics of cellular gain changes will vary across the workspace in a characteristic way. Figure 3 plots the distribution of gain ratios across a population of joint synergy cells at four postures assuming a uniform distribution of internal pds in joint angle space.

Neither Table 1 nor Figure 2 can presently be compared with published data, since nowhere in the literature has the linkage previously been made between a cell's absolute spatial pd at one posture and the gain change that was exhibited between two (or more) postures. Figure 3 cannot yet be compared with published data either since experimentalists have focused on the population statistics of directional shifts as opposed to gain changes.

Gain effects can be represented in a cell's tuning equation by the following modification of the standard cosine model:

$$\upsilon\left(\vec{\omega}_{\mathrm{pd}}(\theta,\varphi)\right) = b_0 + \xi\left\|\vec{\omega}_{\mathrm{pd}}(\theta,\varphi)\right\|\cos\left(\omega - \omega_{\mathrm{pd}}(\theta,\varphi)\right) \qquad (2)$$

where the cell's gain, b_1, has been replaced by a constant component, ξ, and a variable component, $\left\|\vec{\omega}_{\mathrm{pd}}(\theta,\varphi)\right\|$, which is the magnitude of the posture-dependent spatial pd vector denoted as $\vec{\omega}_{\mathrm{pd}}(\theta,\varphi)$. Hereafter, the posture-dependence, (θ,φ), will be implicitly assumed wherever ω_{pd} or $\left\|\vec{\omega}_{\mathrm{pd}}\right\|$ appear but will not be explicitly included in the notation.

Previous studies (Caminiti *et al.*, 1990; Scott and Kalaska, 1997; Kakei *et al.*, 1999) investigated changes in a cell's preferred direction as a means to infer an underlying coordinate system. While variations in gain were noted, they were not identified as critically factoring into the coordinate inference problem. However, for the case of joint angle coordinates applied to the 2-DOF arm, predicted variations in a cell's gain are

Table 1
Predicted gain changes assuming joint angle coordinates for four cells

Referènce pd	θ	φ	Gain: $r = 10$	Gain: $r = 15$	Gain: $r = 25$
180°	1.00	0.00	B_1	$1.50B_1$	$2.50B_1$
60°	0.00	–1.00	B_1	B_1	B_1
30°	–0.71	–0.71	B_1	$1.26B_1$	$1.86B_1$
275°	–0.50	0.86	B_1	$0.92B_1$	$0.60B_1$

Each row corresponds to an individual cell. The first column contains a cell's spatial pd at the reference posture [$(\theta, \varphi) = (30°, 120°)$ corresponding to $(x, y) = (0, 15)$], from which the cell's normalized joint synergy was computed. The components of that synergy (shoulder and elbow) are listed in the next two columns, while the next three columns indicate the predicted gains at three different values of *r*, the distance of the hand from the shoulder. The gain at $r = 10$ is arbitrarily assigned a value of unity and the other two gains are written as multiples of that gain. By reading across the table, one sees that the first cell, whose spatial pd of 180° corresponds to shoulder flexion (with no involvement of the elbow joint), is predicted to possess a gain at $r = 25$ which is 2.5 times greater than the gain at $r = 10$. Such a discrepancy in gains is clearly discernible by experiment. On the other hand, a cell with a spatial pd of 60°, which corresponds to a joint synergy of elbow extension (with no involvement of the shoulder joint), is predicted to possess the same gain at all points in the workspace. Subsequent rows of the table list additional cells with mixed joint synergies and the corresponding predictions of gain changes as a function of *r*. For some cells, the gain increases with increasing values of *r*, while for other cells the gain decreases; thus, some cells are predicted to be strongly tuned in the outer portions of the workspace while other cells are predicted to be strongly tuned at locations proximal to the shoulder.

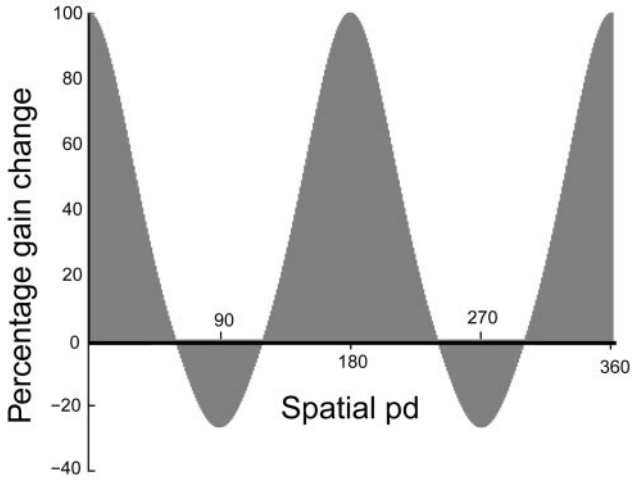

Figure 2. Correlation between spatial pd values and gain changes in a population of joint synergy cells. For a given cell, the gain is evaluated at two different radial distances from the shoulder as the origin. Let G_{10} denote the gain at a distance of 10 cm and G_{20} denote the gain at a distance of 20 cm. For this case, the percent gain change is defined as $((G_{20} - G_{10})/\min(G_{10},G_{20})) \times 100$, so that positive gain changes reflect increasing gains as *r* increases. Percent gain changes are plotted against the spatial pd values at the reference posture in order to illustrate which cells experience which types of gain changes. Note that cells with spatial pds clustered along the horizontal direction tend to exhibit large positive gain changes while cells with spatial pds clustered along the vertical direction tend to exhibit more modest negative gain changes. This plot was constructed for workspace locations at a radial distance of 10 and 20 cm, respectively. If the radial separation were increased, the percent gain changes would be amplified. Note that the percent gain change would be uniformly zero for Cartesian or shoulder-centered coordinates.

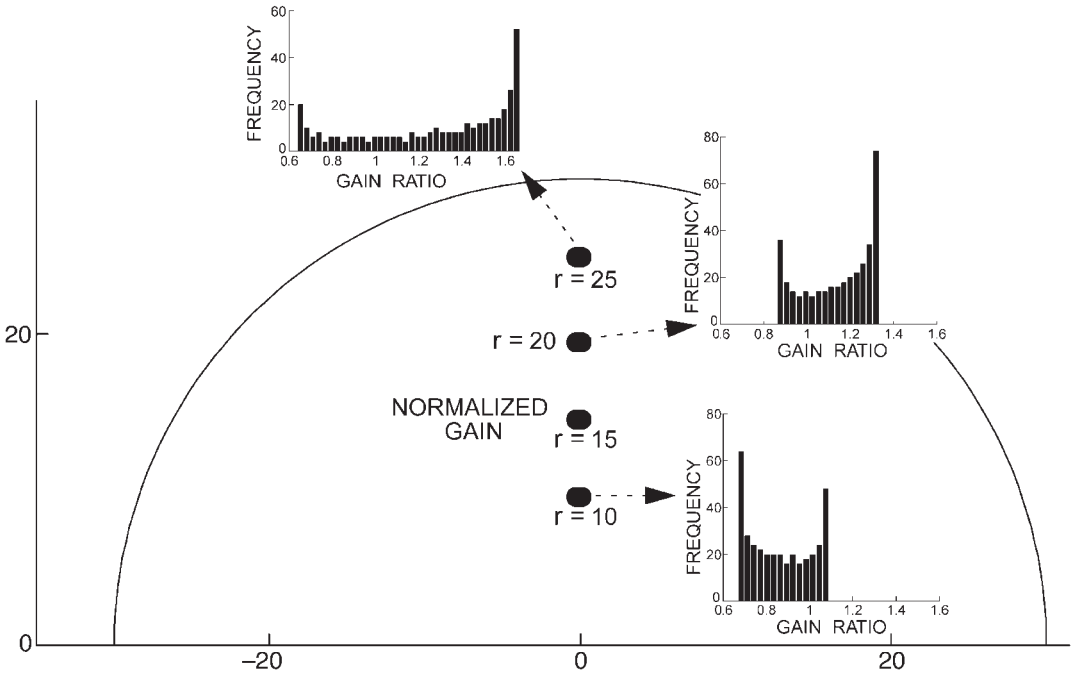

Figure 3. Distribution of gain ratios across four postures in a population of 360 joint synergy cells. A uniform distribution of internal pds in joint angle space was assumed. A cell's gain ratio at a given posture was computed as the ratio of the gain at that posture divided by the gain at a reference posture corresponding to a radial distance of 15 cm between the hand and the shoulder. This procedure automatically normalizes to unity the gains at the reference posture. Note that the gain ratios at all postures would be uniformly 1.0 for Cartesian or shoulder-centered cells.

easier to detect experimentally than predicted shifts in a cell's preferred direction. Specifically, for moderate postural changes (by 'moderate' we mean hand position changes of 10–15 cm), a typical shift in preferred direction is 35–40°. If error bars on preferred direction determinations are on the order of 20°, patterns of directional shifts at the single-cell level may be hard to empirically discern. On the other hand, if one considers gain changes along a radial projection outward from the shoulder, a typical gain change for a moderate postural change stands at a much more distinguishable 50%. Thus, while both directional shifts and gain changes would signify that a transformation into motor coordinates has taken place, gain changes may serve as the more robust indicator for many coordinate systems.

Neurophysiologists have tended to focus on a cell's preferred direction as the chief characteristic of cell response. We have suggested an expanded perspective to response classification whereby a cell's preferred direction and its gain are viewed as dual components of a unitary response vector. By operating on these vector entities, the vector field formalism provides a compact, integrated characterization of how two important cell response properties are predicted to vary across the workspace as a function of posture for any coordinate hypothesis.

Comparison with an Alternative Interpretation of Gain Variability

Although we provide one interpretation for the gain changes observed in motor cortex, other interpretations may apply. For example, Andersen *et al*. reported that the position of the eye in its orbit monotonically modulates the gain of parietal neurons tuned to a preferred retinotopic location (Andersen *et al*. 1985). One interpretation of this phenomenon, supported by computational studies (Grossberg and Kuperstein, 1986; Zipser and Andersen, 1988), is that information about the retinotopic position of the target is combined with eye position information to generate a distributed representation of target location in head-centered coordinates. Analogously, one might imagine that a motor cortical cell, tuned to a directional signal in one coordinate frame, exhibits a gain that is modulated by arm posture to generate a distributed representation of movement direction in a different coordinate frame. While this coordinate-transformational perspective and our vector field framework share features in describing gain changes (see Fig. 4), the two formulations differ conceptually in addressing different functional requirements of the motor control system. The body of work by Anderson and colleagues implicates gain fields as a mechanism for *effecting* coordinate transformations. We propose for M1 that the transformation into some form of motor coordinates has been *completed* and that gain variability arises, as a purely geometric phenomenon, when cells with fixed 'motor actions' are differentially recruited across postures because of the anisotropy of skeletomuscular mechanics. Both types of gain changes could be exhibited by different cells within the same region of cortex, since separate sub-populations of neurons may mediate these separate functions (Kakei *et al*., 1999). However, gain changes that arise from the mechanism we propose will be patterned, at the single-cell level, in accord with a distinct biomechanical signature that is illustrated in Figures 2 and 3 for the specific case of joint angle coordinates.

Speed Effects

Several experimental studies have shown cell activity to correlate with hand speed during multi-joint movements (Schwartz, 1992; Ashe and Georgopoulos, 1994; Moran and Schwartz, 1999a), and several modeling studies have indicated reasons to expect that this speed dependence interacts multiplicatively with the directional component of cell firing rates (Bullock and Grossberg, 1988; Mussa-Ivaldi, 1988; Bullock *et al*., 1998; Zhang and Sejnowski, 1999). To further refine our model of

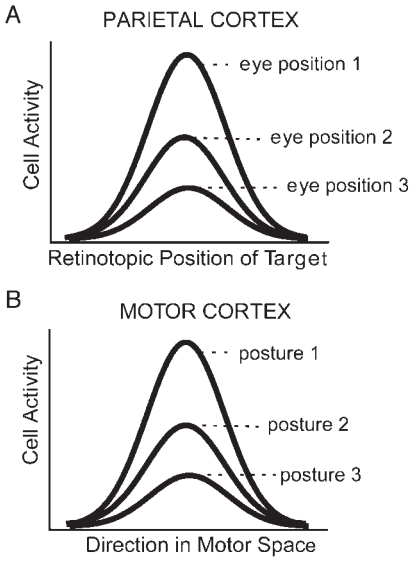

Figure 4. Schematic graphs of two kinds of gain modulation. (*A*) The activity of a subset of parietal (area 7a) neurons is a function of both the target's retinotopic position and the position of the eye in its orbit (Andersen *et al.*, 1985). When the target position is plotted in retinal coordinates — as opposed to the spatial coordinates of the experimentalist's screen — the resulting tuning curves are each centered about the same point, while the gain of the tuning curves is scaled by eye position. This result suggests that information about retinal position and eye position is combined to produce a distributed head-centered representation of target position. (*B*) Motor cortical cells often exhibit posture-dependent spatial pds and posture-dependent gains (Caminiti *et al.*, 1990; Scott and Kalaska, 1997; Kakei *et al.*, 1999). A vector field analysis reveals that if the spatial pds of a cell encoding a motor synergy were plotted in the 'correct' motor coordinates, the resultant tuning curves would all be centered about a single direction that corresponds to a fixed internal pd, and the gains would vary with posture. According to this vector field interpretation and consistent with prior modeling studies (Bullock *et al.*, 1993; Burnod *et al.*, 1999), such gain changes need not imply that the cells in question are themselves mediating a coordinate transformation. For M1 cells showing postural modulation of spatial pds and gains, it is more likely that the transformation into motor coordinates is mediated at a prior sensorimotor stage and that the observed gain variability reflects a dependence of the level of cell recruitment on the (posture-dependent) biomechanical advantage of the cell's action. Other cells, which are mediating a coordinate transformation from spatial into motor coordinates, might exhibit spatial pds that were invariant under postural changes but subject to large posture-dependent gain changes. Kakei *et al*. did find a sub-population of wrist-related, 'extrinsic-like' M1 cells that behave in this manner (Kakei *et al*. 1999).

cortical tuning, we proceed similarly by further decomposing the original coefficient in the cosine model as follows:

$$\upsilon\left(\vec{\omega}_{\mathrm{pd}},\vec{\mathrm{v}}\right) = b_0 + \xi\left\|\vec{\mathrm{v}}\right\|\left\|\vec{\omega}_{\mathrm{pd}}\right\|\cos\left(\omega - \omega_{\mathrm{pd}}\right) \qquad (3)$$

where υ is the instantaneous cell activity at time t, and $\left\|\vec{\mathrm{v}}\right\|$ is the magnitude of the hand velocity vector $\vec{\mathrm{v}}$. Equation (3) indicates that the modulatory component of a cell's firing rate is scaled by the instantaneous hand speed in addition to the variable gain component.

Directional Coding for Arbitrary Trajectories

In work by Schwartz (Schwartz, 1992), monkeys were trained to (i) perform the standard center-out task and (ii) trace a variety of sinusoids. The movement direction varied continuously in the sinusoidal tracing task, and the instantaneous cell activity was found to vary in continuous accord with the angular difference between the movement direction and the preferred direction that was determined in the center-out task. This continuous correlation was not synchronous, but rather cell activity leads that portion of the movement path to which it shows a directional correlation by 100 ms on average (Schwartz, 1992; Ashe and Georgopoulos, 1994; Moran and Schwartz, 1999a), presumably because of the time it takes for a cortical command to be implemented at the periphery. This result suggests that instantaneous cell response may conform to the principles of broad directional tuning about a local preferred direction in arbitrary movement tasks where the movement direction continuously changes. Factoring in this continuous directional correlation and the observed temporal lead, we rewrite equation (3) as:

$$\upsilon\left(\vec{\omega}_{\mathrm{pd}},\vec{\mathrm{v}},t-\tau\right) = b_0 + \xi\left\|\vec{\mathrm{v}}(t)\right\|\left\|\vec{\omega}_{\mathrm{pd}}(t)\right\|\cos\left(\omega(t) - \omega_{\mathrm{pd}}(t)\right) \qquad (4)$$

where t denotes the time at which the hand movement parameters are being measured and τ denotes the temporal offset.

Equation (4) consists of the magnitudes of two vectors (the hand velocity vector and the spatial pd vector) multiplying the cosine of the angle between those vectors. This functional form suggests our final reformulation of the cosine tuning model:

$$\upsilon\left(\vec{\omega}_{\mathrm{pd}},\vec{\mathrm{v}},t-\tau\right) = b_0 + \xi\left(\vec{\omega}_{\mathrm{pd}}(t)\cdot\vec{\mathrm{v}}(t)\right) \qquad (5)$$

Equation (5) indicates that the time-shifted instantaneous firing rate of a cell during arbitrary hand motion equals a movement-related baseline firing rate, b_0 (which is fixed), plus a constant, ξ, times the dot product of the current hand velocity vector, $\vec{\mathrm{v}}$, and the spatial pd vector, $\vec{\omega}_{\mathrm{pd}}$, at the current hand position/posture. Such a dot product formulation of motor cortical cell activity is not original, as it was proposed by Mussa-Ivaldi and by Zhang and Sejnowski (Mussa-Ivaldi, 1988; Zhang and Sejnowski, 1999). However, the present treatment imparts specificity to these generic formulations by interpreting a cell's spatial pd vector as being drawn from a vector field whose structure is determined by an internal coordinate system. Given this specific interpretation, equation (5) by itself captures four firing rate dependencies which characterize a large subset of M1 cells: (i) directional tuning (Georgopoulos *et al.*, 1982; Schwartz *et al.*, 1988); (ii) correlation with hand speed (Schwartz, 1992; Ashe and Georgopoulos, 1994; Moran and Schwartz, 1999a); (iii) variation of spatial pds with hand position (Caminiti *et al.*, 1990) and arm posture (Scott and Kalaska, 1997); and (iv) variation of cellular gains with hand position (Caminiti *et al.*, 1990) and arm posture (Scott and Kalaska, 1997).

Experimental Design for Investigating Coordinates

There are two general methods for capitalizing on differences in vector field structure to attempt to choose between coordinate systems.

Direct Field Sampling

This method consists of determining spatial pd vectors at a reference posture and a small number of other hand positions spread throughout the workspace, as in Figure 1*B–D*, where the thick gray box denotes the reference posture and the smaller thin black boxes denote some other hand locations. On the basis of a cell's spatial pd vector measurement (a direction and a gain) at the reference posture, each coordinate hypothesis makes predictions of the spatial pd vector values (directions and gains) at the other hand positions. These predictions can be compared against the actual spatial pd vector values using least mean-square error analysis to determine the coordinate system of best fit on an individual cell basis.

Indirect Field Sampling

Curved movements that sweep broadly across the workspace visit many postures and so implicitly sample the workspace extensively. With a working model of cell activity over the course of arbitrary trajectories, one can predict, as a function of coordinate choice, the pattern of path-dependent cellular response across multiple curved movement paths and so evaluate alternative coordinate hypotheses. Equation (5) provides such a model. A cell's temporal response profile during the traversal of an arbitrary trajectory can be constructed by: (i) breaking the trajectory into a large number of small, approximately linear, path segments or bins; (ii) determining the movement direction and movement speed within a given bin; and (iii) applying equation (5) to each of these bins. As a result of coordinate-dependent differences in vector field structure, the same movement trajectory will result in a different predicted response profile for different coordinate hypotheses. Below we simulate such a paradigm.

Elliptical Motion

Elliptical motions can illustrate effectively the concept of indirect field sampling. A two-stage experimental protocol [as in (Schwartz, 1992; Moran and Schwartz, 1999b)] is required. In stage 1, the center-out task is run at a reference posture in order to determine a cell's reference spatial pd and its reference gain. In stage 2, cell activity is recorded while an elliptical path is traversed by the hand in both the clockwise and counterclockwise directions. The spatial pd computed in stage 1 enables predictions of a cell's temporal response profiles in stage 2 as a function of coordinate hypothesis, and the predicted response profiles can be compared to the actual response profiles on a cell-by-cell basis to determine the coordinate system of best fit.

Elliptical trajectories offer several advantages in the context of indirect field sampling. First, the instantaneous movement direction over such a path spans the entire angular continuum, thereby ensuring that the response profiles will reflect the full range of directional modulation. Secondly, since elliptical trajectories can be constructed so that the arm visits a broad range of postures within a single movement, alternative coordinate hypotheses will generate highly differentiated response predictions. Thirdly, because of the periodicity of elliptical motion, the animal need not perform a stereotyped movement multiple times (as in the center-out task where a movement in a specific direction is usually repeated five times) but can instead be instructed to extend a unitary movement cycle for multiple periods, thereby facilitating a robust observation of cellular discharge patterns. Finally, since the path curvature changes continuously in a systematic manner over the course of an ellipse, the inverse relationship between curvature and hand speed (Lacquaniti *et al.*, 1983) allows a test of the hypothesis of speed modulation.

For our simulations, we assumed a population of model cells whose spatial pds in a center-out task spanned the angular continuum and whose gains assumed a broad range of values. Subsequently, given the parameters of a specific cell's tuning curve, the cell's temporal response profiles were simulated for each coordinate hypothesis during both counterclockwise and clockwise traversal of the ellipse. The speed profile of the hand was modeled using the two-thirds power law (Lacquaniti *et al.*, 1983), which relates path curvature to instantaneous movement velocity. Figure 5 shows the elliptical path, the curvature along that path, and the velocity profile of the simulated movements. Other details of the simulations are in the Appendix.

Alternative coordinate hypotheses generated, for the same

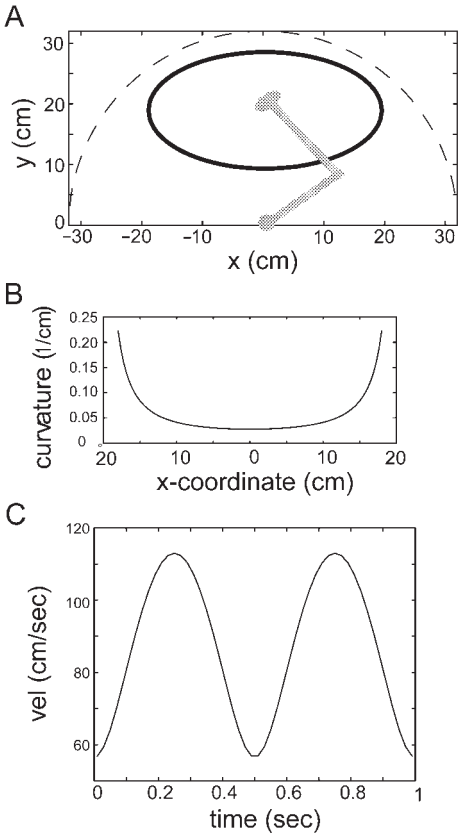

Figure 5. Elliptical motion. (*A*) The spatial configuration of the ellipse. Its traversal is simulated in both the clockwise and counterclockwise directions. The dashed arc indicates the bounds of the workspace. (*B*) A plot of path curvature as a function of *x*-coordinate for the ellipse. (*C*) Tangential velocity profile of the hand as it traverses one complete cycle of the ellipse starting from its right vertex. The speed is calculated from the curvature by means of the two-thirds power law, the application of which requires a constant of proportionality. We chose a constant such that the periphery of the ellipse (with an arclength of 87 cm) was traversed in 1 s for an average speed of 87 cm/s. If such an experiment were performed, the actual speed profiles could be measured.

cell, radically different response predictions in the elliptical tracing task. For example, suppose a cell has the following tuning curve at the reference posture:

$$\upsilon(\omega) = 30 + 20\cos(\omega - 0°)$$

that is, 0 is the cell's preferred direction in degrees (the direction of the spatial pd vector), 20 imp./s is the cell's gain (proportional to the magnitude of the spatial pd vector), and 30 imp./s is the cell's mean movement-related activity (assumed as a constant in this model but given a value for specificity). Figure 6*A* plots predicted temporal response profiles for this cell under the assumption of Cartesian spatial coordinates and joint angle coordinates during two cycles of counterclockwise traversal of the elliptic path. Although both response profiles are roughly sinusoidal with the same phase, two distinct response differences emerge from the plots. First, the joint angle coordinate hypothesis leads to a significantly greater modulation in firing rate. The difference between the maximum and minimum firing rates is 40 imp./s for joint angle coordinates as opposed to 30 imp./s for Cartesian spatial coordinates. Secondly, the mean firing rate during the task is depressed under the assumption of joint angle coordinates (21 imp./s) as compared to Cartesian spatial coordinates (30 imp./s). Note that the baseline level of

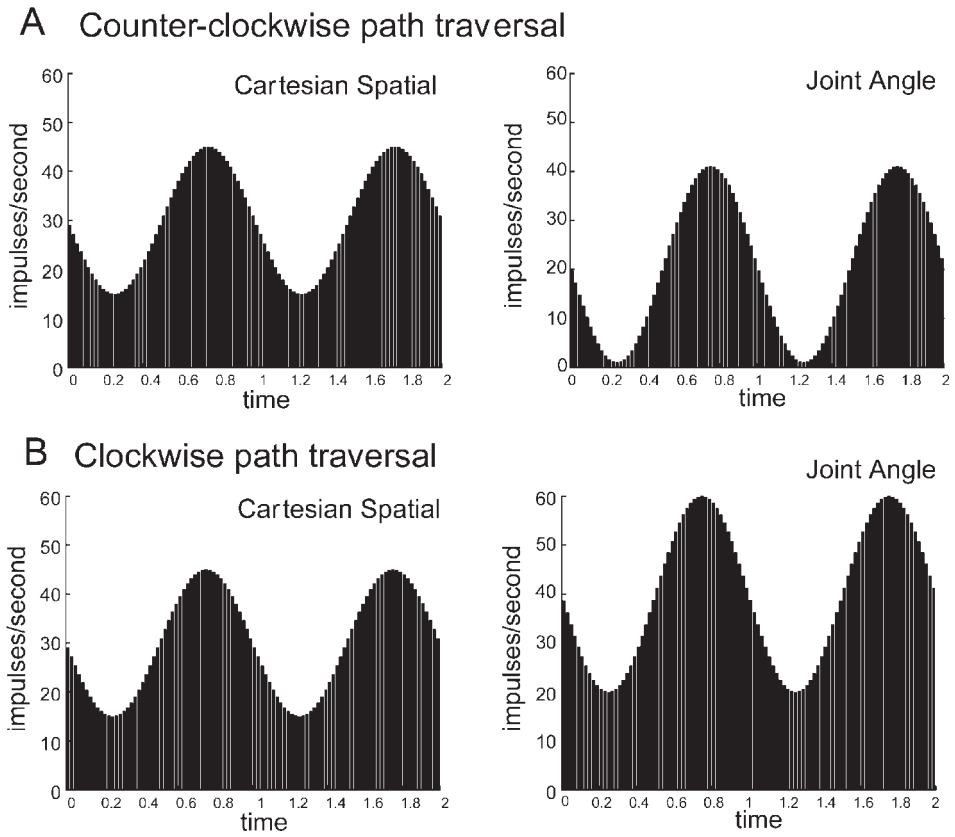

Figure 6. Predicted response profiles under two coordinate hypotheses for a sample cell whose tuning curve at the reference posture is taken to be $\upsilon(\omega) = 30 + 20\cos(\omega - 0°)$. (*A*) Response profiles when the ellipse is traversed in the counterclockwise direction under the assumption of both Cartesian spatial and joint angle coordinates. (*B*) Response profiles when the ellipse is traversed in the clockwise direction under the assumption of both coordinate systems. Different coordinate hypotheses lead to different levels of response alteration under trajectory reversal. Under the assumption of Cartesian spatial coordinates, the response profile remains the same upon direction reversal, while under the assumption of joint angle coordinates, the baseline of the response profiles increases significantly from 21 imp./s for the counterclockwise path to 39 imp./s for the clockwise path.

movement-related activity as determined through the center-out task, b_0, has not changed; rather, the new task engenders different mean levels of task response depending on the coordinate hypothesis.

Simulation results also showed that coordinate-dependent differences in cell response were strikingly accentuated by reversing the direction of path traversal from counterclockwise to clockwise. While trajectory reversal did not change the mean activity level of any cell under the assumption of Cartesian spatial coordinates, the mean activity level did shift and sometimes shifted dramatically for the case of joint angle coordinates (compare Fig. 6*A* with Fig. 6*B*). The Appendix provides an explanation as to why these shifts arise.

All cells exhibited differences, often quite pronounced, in their response properties as a function of coordinate system, although the form of the differences varied from cell to cell. For some cells, the mean level of cell response was similar under the alternative coordinate hypotheses but other aspects of its response profiles – such as the number of peaks, the level of task modulation, the overall profile shape, etc. – differed radically (see Fig. 7). While there exists no simple manner for codifying response profile differences as a function of coordinate hypothesis, the Appendix notes some overall features that were observed to hold.

Population Distributions of Preferred Directions

Just as the assumption of an internal coordinate system can predict variations in the preferred direction of an individual cell, so too can it predict variations in the distribution of preferred directions over a population of directionally tuned cells. The single-cell analysis required an instance of a cell's spatial pd at a reference posture; analogously, the population level analysis requires a determination of the *distribution* of preferred directions at a reference posture. Some studies have revealed distributions which are unimodal (Georgopoulos *et al*., 1982) or bimodal (Scott and Kalaska, 1997) while others have demonstrated a more uniform distribution (Lurito *et al*., 1991). Although none of these studies confined arm motion to within the task plane, as is the case for our model 2-DOF planar arm, a roughly uniform distribution of preferred directions at a central posture seems like a reasonable assumption. We adopt this assumption in our simulations, but the vector field approach can analyze distributional variations associated with any distribution that is found at a reference posture.

Under the assumption of Cartesian spatial coordinates, a cell's preferred direction does not change throughout the workspace; therefore, the population distribution of preferred directions does not change. Under the assumption of shoulder-centered coordinates, a cell's preferred direction does rotate, but since each cell's preferred direction rotates by an equal amount, the population distribution remains unchanged. When joint angle coordinates are assumed, however, significant alterations in the population distribution will occur since the Jacobian rotates joint angle velocity vectors in a highly non-uniform manner. Figure 8*A* plots the distributions of preferred directions at six workspace locations for a sample population exhibiting a

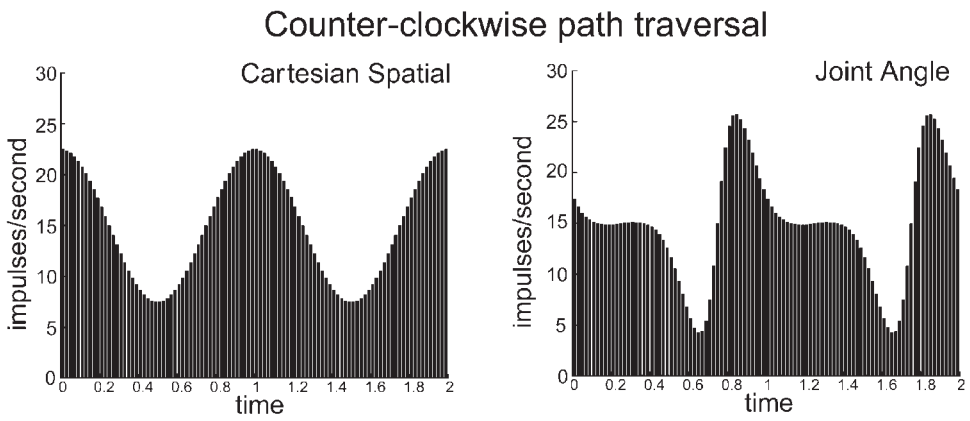

Figure 7. Predicted profile for another cell under two coordinate hypotheses during counter- clockwise motion. The tuning curve for this cell is $\upsilon(\omega) = 15 + 20\cos(\omega - 90°)$. Note how the joint angle response demonstrates greater modulation and sharper burst-like properties than the Cartesian spatial response, although the effective baselines are roughly equal.

uniform distribution at a central posture. Each distribution is represented by a polar histogram plot. The uniform distribution at the reference posture becomes skewed in a systematic and geometrically structured manner as a function of workspace location. The Appendix derives the properties of the skewing through an analysis of symmetries in the Jacobian matrix.

In generating Figure 8*A*, a uniform distribution of spatial pds at the reference posture is transformed into a distribution of internal pds. This internal distribution, plotted in Figure 8*B* in a coordinate system whose axes correspond to shoulder and elbow rotation rates, will not be uniform because it was generated by application of the inverse Jacobian. A 'direction' in the coordinate system of Figure 8*B* indicates the relative shoulder and elbow components of the joint synergy to which a cell is tuned. As the plot shows, the most prevalent joint synergies are those composed of equal parts shoulder extension and elbow flexion or those composed of equal parts shoulder flexion and elbow extension. Synergies consisting of roughly equal percentages of shoulder and elbow extension or of shoulder and elbow flexion are less numerous, as are synergies corresponding primarily to single joint rotation. Since bi-articular muscles induce the same type of rotation in both spanned joints, their action alone could not produce this type of a distribution. Instead, if such a distribution were to exist in the internal space, some higher level functional grouping would be implied whereby flexor muscles for one joint and extensor muscles for the other joint are synergistically innervated through the action of individual cortical neurons.

Although we assumed a uniform distribution of spatial preferred directions at a reference posture, we could alternatively posit a uniform distribution in the internal space and compute the corresponding spatial distributions. Figure 9*B* shows the spatial pd distributions that result from the assumption of uniformity in the internal space (depicted in Fig. 9*A*). Note that the distributions in Figure 9*B* are more highly skewed than the distributions in Figure 8*A*. In fact, the spatial distributions generated by the assumption of a uniform internal distribution never themselves approach uniformity and, with the exception of a small range of hand placements close to the shoulder, are everywhere more skewed than their counterparts in Figure 8*A* (see the Appendix for details). Therefore, if a uniform spatial distribution is revealed at any point in the workspace and if joint angle coordinates are hypothesized, then the underlying internal distribution must be significantly skewed. Further, a finding of uniform spatial distributions throughout the workspace would provide support for the hypothesis of a spatially based coordinate system.

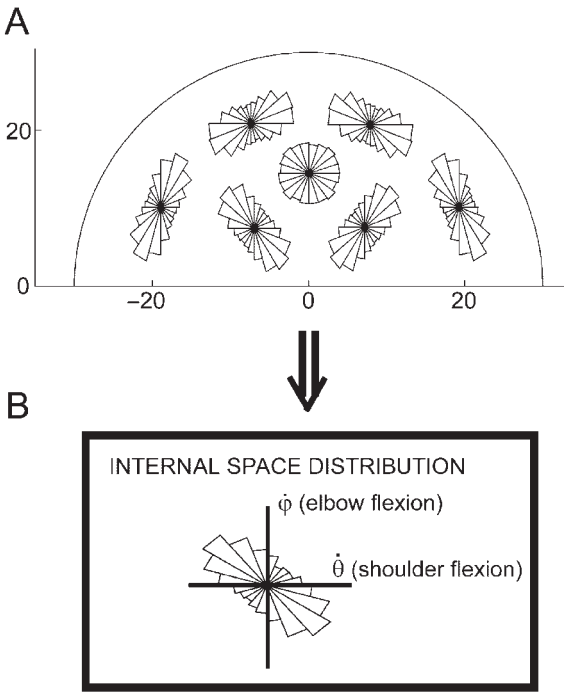

Figure 8. Distributions of spatial pds assuming spatial uniformity. (*A*) Polar plots of the distributions of spatial pds at six different workspace locations assuming a uniform spatial distribution at a central reference posture. The distributions vary in an orderly and symmetrical fashion that reflects the underlying symmetries of the Jacobian when the upper and lower arm segments are roughly equal in length. (*B*) The corresponding internal distribution of cells that engenders a uniform distribution at the reference posture. Note the pronounced asymmetry in joint angle space with a bias towards the axis that corresponds to opposing motions about the two joints. Motion along that axis could not be induced by cells which activated individual bi-articular muscles since such muscles will induce either flexion or extension about both joints. Instead, if such an internal distribution actually exists, some higher level modularization of the motor periphery, possibly mediated by the spinal circuitry, would be required to generate a prevalence of joint synergies along the axis indicated.

Population Vector Encoding

The distributions shown in Figures 8*A* and 9*B* are bimodal and,

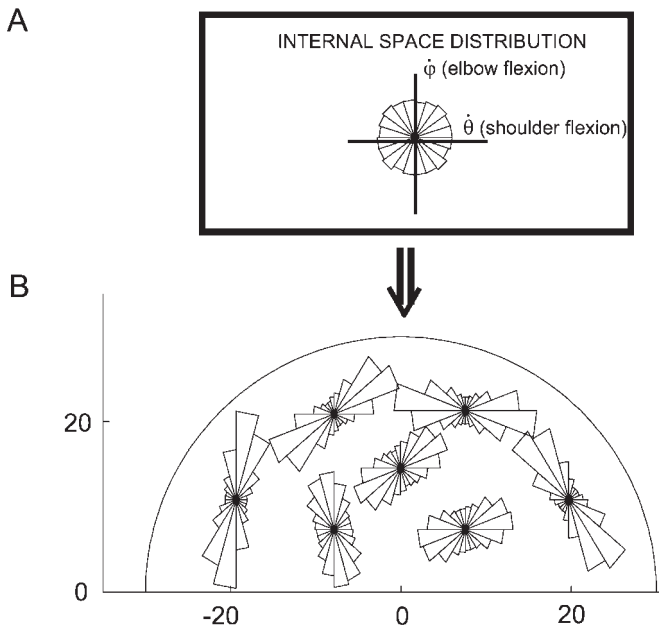

Figure 9. Distributions of spatial pds assuming uniformity in joint angle space. (*A*) The polar plot of a uniform distribution of pds in joint angle space. (*B*) The spatial pd distributions at the same workspace locations as in Figure 8*A* when a uniform distribution in the internal space is assumed. These distributions are generally more skewed than their counterparts in Figure 8*A*. Even the distribution at the central reference posture demonstrates a strong bias. Ultimately, the spatial pd distributions must be determined empirically, although coordinate analysis can determine whether the variation of distributions across the workspace is consistent with a particular coordinate hypothesis.

hence, do not conform to the criteria necessary to guarantee that the population vector direction (Georgopoulos *et al*., 1983) is colinear with the movement direction (Georgopoulos *et al*., 1988; Mussa-Ivaldi, 1988; Sanger, 1994). Despite the strong bimodality, however, the population vector algorithm remains a good predictor of movement direction. See the Appendix for details.

Discussion

Formulating explicit models of cell firing rates as a function of global movement variables remains a daunting task given the manifold functional dependencies exhibited by cortical cells in a variety of behavioral contexts (see Introduction). This paper restricts the analysis to the representation of movement direction and speed which together constitute a unitary physical entity, the movement velocity vector. A cell's preferred direction and the depth of modulation of its directional tuning curve – two experimentally determined parameters commonly used to describe the encoding of direction – can be viewed as dual aspects of a single spatial pd vector. If individual cell activity encodes movement information in a fixed internal coordinate system, the pattern by which a cell's spatial pd vector varies across the workspace serves as a signature of those underlying coordinates. Finally, a model was proposed of cell firing during the traversal of an arbitrary trajectory. In this unified model, the instantaneous level of cell discharge depends upon the dot product of a cell's local, posture-dependent, spatial pd vector (drawn from a vector field of spatial pds) and the current hand movement vector.

Both Lacquaniti *et al*. and Scott and Kalaska have investigated the movement-related responses of neurons under different coordinate hypotheses including joint-based representations (Lacquaniti *et al*., 1995; Scott and Kalaska, 1997). We have generalized upon their methodologies to (i) incorporate gain changes, as well as directional shifts, in tackling the coordinate inference problem with respect to arbitrary coordinate systems; (ii) include the dependence of cell firing rates on hand speed; and (iii) consider how population distributions of preferred directions will systematically change. But even as the methodology of this paper is designed to elucidate 'the' coordinate system in which a single cell encodes its movement information, no guarantee exists that cells utilize invariant coding strategies across diverse movement tasks. In fact, accumulating evidence for representational plasticity (Wise *et al*., 1998; Gandolfo *et al*., 2000), combined with the profound overtraining that occurs in neurophysiological studies, suggests that motor control problems are solved by the adoption of task-dependent strategies, which utilize task-dependent coordinate decompositions of the sensorimotor transformation. Viewed from this perspective, the implication of a particular representational scheme in a cell's response during a specific task need not signify a functionally invariant role for that cell within the overall motor circuit.

The computational techniques, developed here for the analysis of arm movements, can be extended to a consideration of wrist movements or other end-effector motions. Recently, Kakei *et al*. (Kakei *et al*., 1999) conducted a comprehensive direct-sampling study in which the preferred directions of wrist-related motor cortical cells during the final 100 ms before movement onset were determined in three different wrist postures: pronated, supinated, and mid (halfway between the two). On the basis of the shifts in spatial pds, most cells were grouped into two different categories: a large class of extrinsic-like cells, which exhibited relatively small shifts in pds across postures, and a smaller class of muscle-like cells, which exhibited shifts in pds similar to the shifts of individual muscle pds determined from EMG activity. In light of previous results on M1 cells involved in wrist movements (Evarts, 1968; Cheney and Fetz, 1980) and arm movements (Scott and Kalaska, 1997), and given the more focused pattern of connectivity from wrist-related M1 cells to alpha motoneurons when compared to arm-related M1 cells (Kuypers, 1981), the excess of extrinsic-like cells over muscle-like cells in Kakei *et al*. (Kakei *et al*., 1999) may seem surprising.

Kakei *et al.* (Kakei *et al.*, 1999), however, did not factor gain changes into their formulation of coordinate system hypotheses. In fact, 61% of the extrinsic-like cells were found to exhibit significant shifts in gain, a number similar to both the 66% of muscle-like cells that exhibited gain changes and the 74% of forearm muscles that exhibited gain changes in their EMG activity. From the vector field perspective, such marked cellular gain changes themselves indicate that a transformation into muscle-based coordinates may have already occurred. This hypothesis may be further supported by the finding that response properties other than pds shifts (such as onset latency, threshold for evoking muscle contraction, and general profile shape) were similar between the two cell populations. Nevertheless, it remains to be seen whether a muscle-based explanation of the Kakei *et al*. data (Kakei *et al*., 1999) can engender the clearly bimodal distribution of pd shifts that was observed.

The activity of many proximal arm-related M1 cells is modulated in response to variable force conditions imposed upon the arm during movement (Kalaska *et al*., 1989; Sergio and Kalaska, 1998; Gandolfo *et al*., 2000). While this paper's analysis focused purely on kinematic coordinate systems, the vector field framework can also be used to investigate hypotheses that

motor cortical cells encode muscle force or muscle activation. However, to perform such an analysis requires knowledge of the posture-dependent inertial, viscous, and elastic forces involved in center-out hand movements, as well as a detailed biomechanical muscle model and an understanding of cortical recruitment patterns. Obtaining reliable information of this type remains an area of ongoing research. Todorov (Todorov, 2000) developed a model of the direct cortical activation of muscles by making rough assumptions about the relevant forces and by restricting the scope of the model to a local analysis conducted in spatial coordinates. Based on the simple premise that M1 cells provide a feedforward prediction of the muscle activation necessary to generate the state-dependent muscle forces required for task performance, the model of Todorov (Todorov, 2000) addresses a wide array of experimental results in a parsimonious manner. However, because Todorov (Todorov, 2000) is a population-level model and because the model, constructed as a local analysis, does not take into account the effects of skeletomuscular geometry, it cannot clarify nor make predictions of posture-dependent changes in single-cell response properties. From the perspective of this paper, such variations in response properties are crucial for investigating functional hypotheses, not just about the role of M1 pyramidal tract neurons, but about the role of neurons in non-primary motor areas, parietal areas, and other brain regions implicated in the sensorimotor transformation.

Beyond making inferences on the basis of any specific dataset, the analytic framework we propose strives for a refined single-cell approach to representational issues in motor neurophysiology. In the past, analyses have largely been predicated on the population statistics of cell correlations with movement variable(s). The methodology of this paper points toward further studies where detailed information about neuroanatomy, skeletomuscular geometry, and movement kinematics/dynamics is comprehensively integrated with functional hypotheses about the role of distinct cell sub-populations to investigate single-cell response across a variety of movement tasks.

Notes

This work was supported by the Defense Advanced Research Projects Agency (ONR N00014-92-J-4015), the Defense Advanced Research Projects Agency and the Office of Naval Research (ONR N00014-95-1-0409), the National Science Foundation (NSF IRI-90-00 530 and NSF IRI-97-20 333), and the Office of Naval Research (ONR N00014-91-J-4100, ONR N00014-92-J-1309, ONR N00014-94-1-0940, and ONR N00014-95-1-0657). The authors would like to thank Mukund Balasubramanian and Paul Cisek for their comments about the work. This is technical report CAS/CNS-2000-017.

Address correspondence to Daniel Bullock or Stephen Grossberg, Department of Cognitive and Neural Systems, Boston University, 677 Beacon Street, Boston, MA 02215, USA. Email: danb@cns.bu.edu or steve@cns.bu.edu.

References

Ajemian R, Bullock D, Grossberg S (2000) Kinematic coordinates in which motor cortical cells encode movement direction. J Neurophysiol 84:2191–2203.

Alexander GE, Crutcher MD (1990a) Preparation for movement: neural representations of intended direction in three motor areas of the monkey. J Neurophysiol 64:133–150.

Alexander GE, Crutcher MD (1990b) Neural representations of the target (goal) of visually guided arm movements in three motor areas of monkey. J Neurophysiol 64:164–178.

Andersen RA, Essick GK, Siegel RM (1985) Encoding of spatial location by posterior parietal neurons. Science 230:456–458.

Ashe J, Georgopoulos AP (1994) Movement parameters and neural activity in motor cortex and area 5. Cereb Cortex 6:590–600.

Bullock D, Grossberg S (1988) Neural dynamics of planned arm movements: emergent invariants and speed–accuracy properties during trajectory formation. Psychol Rev 95:49–90.

Bullock D, Grossberg S, Guenther FH (1993) A self-organizing neural model of motor equivalent reaching and tool use by a multijoint arm. J Cogn Neurosci 5:408–435.

Bullock D, Cisek P, Grossberg S (1998) Cortical networks for control of voluntary arm movements under variable force conditions. Cereb Cortex 8:48–62.

Burnod Y, Baraduc P, Battaglia-Mayer A, Guigon E, Koechlin E, Ferraina S, Lacquaniti F, Caminiti R (1999) Parieto-frontal coding of reaching: an integrated framework. Exp Brain Res 129:325–346.

Caminiti R, Johnson PB, Urbano A (1990) Making arm movements within different parts of space: dynamic aspects in the primate motor cortex. J Neurosci 10:2039–2058.

Carpenter AF, Georgopoulos AP, Pellizzer G (1999) Motor cortical encoding of serial order in a context-recall task. Science 283: 1752–1757.

Craig, JJ (1986) Introduction to robotics: mechanics and control. Reading, MA: Addison-Wesley.

Cheney PD, Fetz EE (1980) Functional classes of primate corticomotoneuronal cells and their relation to active force. J Neurophysiol 44:773–791.

Crutcher MD, Alexander GE (1990) Movement-related neuronal activity selectively coding either direction or muscle pattern in three motor areas of the monkey. J Neurophysiol 64:151–163.

Evarts EV (1968) Relation of pyramidal tract activity to force exerted during voluntary movement. J Neurophysiol 31:14–27.

Fu Q-G, Suarez JI, Ebner TJ (1993) Neuronal specification of direction and distance during reaching movements in the superior precentral premotor area and primary motor cortex of monkeys. J Neurophysiol 70:2097–2116.

Fu Q-G, Flament D, Coltz JD, Ebner TJ (1995) Temporal encoding of movement kinematics in the discharge of primate primary motor and premotor neurons. J Neurophysiol 73:836–854.

Gandolfo F, Li CR, Benda BJ, Schioppa CP, Bizzi E (2000) Cortical correlates of learning in monkeys adapting to a new dynamical environment. Proc Natl Acad Sci USA 97:2259–2263.

Georgopoulos AP, Kalaska JF, Caminiti R, Massey JT (1982) On the relations between the direction of two-dimensional arm movements and cell discharge in primate motor cortex. J Neurosci 2:1527–1537.

Georgopoulos AP, Caminiti R, Kalaska JF, Massey JT (1983) Spatial coding of movement: a hypothesis concerning the coding of movement direction by motor cortical populations. Exp Brain Res Suppl 7: 327–336.

Georgopoulos AP, Caminiti R, Kalaska JF (1984) Static spatial effects in motor cortex and area 5: quantitative relations in a two-dimensional space. Exp Brain Res 54:446–454.

Georgopoulos AP, Kettner RE, Schwartz AB (1988) Primate motor cortex and free arm movements to visual targets in three-dimensional space. II. Coding of the direction of movement by a neuronal population. J Neurosci 8:2928–2937.

Georgopoulos AP, Ashe J, Smyrnis N, Taira M (1992) The motor cortex and the coding of force. Science 256:1692–1695.

Grossberg S, Kuperstein M (1986) Neural dynamics of adaptive sensory–motor control. New York: Elsevier Science.

Kakei S, Hoffman DS, Strick PL (1999) Muscle and movement representations in the primary motor cortex. Science 285:2136–2139.

Kalaska JF, Hyde, ML (1985) Area 4 and area 5: differences between the load direction-dependent discharge variability of cells during active postural fixation. Exp Brain Res 59:197–202.

Kalaska JF, Cohen DAD, Hyde ML, Prud'homme M (1989) A comparison of movement direction-related versus load direction-related activity in primate motor cortex, using a two-dimensional reaching task. J Neurosci 9:2080–2102.

Kettner RE, Marcario JK (1996) Control of remembered reaching sequences in monkey. II. Storage and preparation before movement in motor and premotor cortex. Exp Brain Res 42:223–227.

Kettner RE, Schwartz AB, Georgopoulos AP (1988) Primate motor cortex and free arm movements to visual targets in three-dimensional space. III. Positional gradients and population coding of movement direction from various movement origins. J Neurosci 8:2938–2947.

Kuypers HG (1981) Anatomy of the descending pathways. In: Handbook of physiology. The nervous system II (Brooks VB, ed.), pp. 597–666. Bethesda, MD: American Physiological Society.

Lacquaniti F, Terzuolo C, Viviani P (1983) The law relating the kinematic and figural aspects of drawing movements. Acta Psychol (Amst) 54:115–130.
Lacquaniti F, Guigon E, Bianchi L, Ferraina S, Caminiti R (1995) Representing spatial information for limb movement: role of area 5 in the monkey. Cereb Cortex 5:391–409.
Lurito JT, Georgakopoulos T, Georgopoulos AP (1991) The making of movements at an angle from a stimulus direction: studies of motor cortical activity at the single cell and population levels. Exp Brain Res 87:562–580.
Moran DW, Schwartz AB (1999a) Motor cortical representation of speed and direction during reaching. J Neurophysiol 82:2676–2692.
Moran DW, Schwartz AB (1999b) Motor cortical activity during drawing movements: population representation during spiral tracing. J Neurophysiol 82:2693–2704.
Mussa-Ivaldi FA (1988) Do neurons in the motor cortex encode movement direction? An alternate hypothesis. Neurosci Lett 91:106–111.
Sanger TD (1994) Theoretical considerations for the analysis of population coding in motor cortex. Neural Computation 6:29–37.
Schwartz AB (1992) Motor cortical activity during drawing movements: single unit activity during sinusoid tracing. J Neurophysiol 68: 528–541.
Schwartz AB (1993) Motor cortical activity during drawing movements: population representation during sinusoid tracing. J Neurophysiol 70:28–36.
Schwartz AB (1994) Direct cortical representation of drawing. Science 265:540–542.
Schwartz AB, Kettner RE, Georgopoulos AP (1988) Primate motor cortex and free arm movements to visual targets in 3-d space. I. Relations between single cell discharge and direction of movement. J Neurosci 8:2913–2927.
Scott SH, Kalaska JF (1997) Reaching movements with similar hand paths but different arm orientations. I. Activity of individual cells in motor cortex. J Neurophysiol 77:826–852.
Sergio LE, Kalaska JF (1997) Systematic changes in directional tuning of motor cortex cell activity with hand location in the workspace during generation of static isometric forces in constant spatial directions. J Neurophysiol 78:1170–1174.
Sergio LE, Kalaska JF (1998) Changes in the temporal pattern of primary motor cortex activity in a directional isometric force versus limb movement task. J Neurophysiol 80:1577–1583.
Shen L, Alexander GE (1997) Neural correlates of a spatial sensory-to-motor transformation in primary motor cortex. J Neurophysiol 77:826–852.
Taira M, Boline J, Smyrnis N, Georgopoulos AP, Ashe J (1996) On the relations between single cell activity in the motor cortex and the direction and magnitude of three-dimensional static isometric force. Exp Brain Res 109:367–376.
Tanaka S (1994) Hypothetical joint-related coordinate systems in which populations of motor cortical neurons code direction of voluntary arm movements. Neurosci Lett 180:83–86.
Todorov E (2000) Direct cortical control of muscle activation in voluntary arm movements: a model. Nat Neurosci 3:391–398.
Wise SP, Moody SL, Blomstrom KJ, Mitz AR (1998) Changes in motor cortical activity during visuomotor adaptation. Exp Brain Res 121:285–289.
Zhang K, Sejnowski TJ (1999) A theory of geometric constraints on neural activity for natural three-dimensional movement. J Neurosci 19: 3122–3145.
Zipser D, Andersen RA (1988) A back-propagation programmed network that simulates response properties of a subset of posterior parietal neurons. Nature 331:679–684.

Appendix: the Posture-dependent Gain of a Cell Encoding a Joint Synergy

For the standard 2-DOF arm [e.g. see (Craig, 1986)], the forward kinematic equations are:

$$x = k_1 \cos\theta + k_2 \cos(\theta + \varphi) \tag{A1}$$

$$y = k_1 \sin\theta + k_2 \sin(\theta + \varphi) \tag{A2}$$

where x and y denote Cartesian end-effector coordinates, θ and φ denote the shoulder and joint angles, k_1 and k_2 denote the lengths of the proximal and distal arm segments. The Jacobian is:

$$J(\theta,\varphi) = \begin{pmatrix} -k_1 \sin(\theta) - k_2 \sin(\theta+\varphi) & -k_2 \sin(\theta+\varphi) \\ k_1 \cos(\theta) + k_2 \cos(\theta+\varphi) & k_2 \cos(\theta+\varphi) \end{pmatrix} \tag{A3}$$

which can be rewritten in a compact form that involves end-effector coordinates and joint angles:

$$J(\theta,\varphi) = \begin{pmatrix} -y & -k_2 \sin(\theta+\varphi) \\ x & k_2 \cos(\theta+\varphi) \end{pmatrix} \tag{A4}$$

Denote a cell's internal pd or normalized joint synergy as $\begin{pmatrix} \dot{\theta}^*_{pd} \\ \dot{\varphi}^*_{pd} \end{pmatrix}$. Multiplying this synergy by the Jacobian yields the following spatial pd vector:

$$\begin{pmatrix} \dot{x} \\ \dot{y} \end{pmatrix} = \begin{pmatrix} -y\dot{\theta}^*_{pd} - k_2 \sin(\theta+\varphi)\dot{\varphi}^*_{pd} \\ x\dot{\theta}^*_{pd} + k_2 \cos(\theta+\varphi)\dot{\varphi}^*_{pd} \end{pmatrix} \tag{A5}$$

The magnitude of this spatial pd vector, which is proportional to the cellular gain, is:

$$\left\|\vec{\omega}_{pd}(x,y)\right\| = \sqrt{\left(-y\dot{\theta}^*_{pd} - k_2 \sin(\theta+\varphi)\dot{\varphi}^*_{pd}\right)^2 + \left(x\dot{\theta}^*_{pd} + k_2 \cos(\theta+\varphi)\dot{\varphi}^*_{pd}\right)^2} \tag{A6}$$

Expanding the above expression and combining terms leaves:

$$\left\|\vec{\omega}_{pd}\right\| = \sqrt{r^2\dot{\theta}^{*\,2}_{pd} + k_2^2\dot{\varphi}^{*\,2}_{pd} + 2k_2\dot{\theta}^*_{pd}\dot{\varphi}^*_{pd}\left(x\cos(\theta+\varphi) + y\sin(\theta+\varphi)\right)} \tag{A7}$$

where $r = \sqrt{x^2 + y^2}$. With equations (A1) and (A2, A7) simplifies to:

$$\left\|\vec{\omega}_{pd}\right\| = \sqrt{r^2\dot{\theta}^{*\,2}_{pd} + k_2^2\dot{\varphi}^{*\,2}_{pd} + 2k_2\dot{\theta}^*_{pd}\dot{\varphi}^*_{pd}\left(k_1\cos\varphi + k_2\right)} \tag{A8}$$

Using the inverse kinematic equation for φ eliminates joint angles from the expression for gain:

$$b_1 \propto \sqrt{r^2\dot{\theta}^{*\,2}_{pd} + k_2^2\dot{\varphi}^{*\,2}_{pd} + r^2\dot{\theta}^*_{pd}\dot{\varphi}^*_{pd} - k_1^2\dot{\theta}^*_{pd}\dot{\varphi}^*_{pd} + k_2^2\dot{\theta}^*_{pd}\dot{\varphi}^*_{pd}} \tag{A9}$$

For the rest of the Appendix, go to http://www.cns.bu.edu/pub/ajemian.